ELSEVIER

Journal of Photochemistry and Photobiology A: Chemistry 152 (2002) 95–101

Journal of Photochemistry and Photobiology A:Chemistry

www.elsevier.com/locate/jphotochem

Reaction mechanism of thymine dimer formation in DNA induced by UV light

Bo Durbeej [a,b], Leif A. Eriksson [b,*]

[a] *Department of Quantum Chemistry, Box 518, Uppsala University, S-75120 Uppsala, Sweden*
[b] *Department of Biochemistry, Box 576, Uppsala University, S-75123 Uppsala, Sweden*

Received 15 February 2002; received in revised form 25 April 2002; accepted 7 May 2002

Abstract

The formation of thymine dimers in DNA is investigated by means of density functional theory (DFT) techniques. While it is found that a thermally induced [2 + 2] cycloaddition reaction proceeds via a very high energy transition state (80–88 kcal/mol above the reactant complex), the energy barrier for UV light induced formation—explored within the time-dependent DFT formalism—is only a few kilocalories per mol. As such, these results serve as an illustrative example of how UV radiation may induce DNA lesions. For the reactant complex, the calculated vertical excitation energy corresponding to the $S_1 \leftarrow S_0$ transition ($\pi \rightarrow \pi^*$) lies in the far-UV region, in accordance with experimental data.

Keywords: Time-dependent density functional theory; UV light; Thymine dimer formation; Excitation energies

1. Introduction

Exposure of DNA to UV radiation has a mutagenic effect on cellular systems. A major type of UV light induced damage is the formation of cyclobutane pyrimidine dimers (Pyr<>Pyr) between adjacent pyrimidine bases in DNA exposed to UV radiation in the range of 200–300 nm (far-UV) [1,2]. These lesions are harmful to cells since they inhibit the enzymes carrying out DNA replication and transcription, and are believed to be the main source of carcinogenic mutations due to miscoding during replication.

Repair of damaged DNA occurs either by photoreactivation through concurrent or subsequent exposure to near-UV and visible light (300–500 nm), or by nucleotide- or base-excision repair pathways [3–5]. In the photoreactivation process, the Pyr<>Pyr dimers are restored back into individual pyrimidine bases in a reaction catalyzed by the enzyme DNA photolyase (Fig. 1). The commonly accepted model for the photorepair mechanism proposes that the dimer splitting is a consequence of a single electron transfer from the enzyme to the dimer [6–8]; a mechanism recently verified by quantum chemical calculations [9].

Several experimental and theoretical studies are available in which the effects of the Pyr<>Pyr dimers on the overall structure of DNA dodecamers are investigated. NMR studies and melting temperature measurements have revealed that the *cis–syn* stereoisomer—the predominant stereoisomer found in UV irradiated DNA—invokes a highly localized kink to the DNA strand, and also displays mismatched hydrogen bonding with the complementary strand primarily at the 5′ end of the damage [10,11]. These structural features have been well reproduced by several groups by means of molecular dynamic simulations [12,13].

Albeit the structural effects of the Pyr<>Pyr dimers on DNA are fairly well understood, there have been no detailed investigations reported on the exact mechanism leading to their formation. The reaction between the two bases may be described either as a [2+2] cycloaddition, or as a pyrimidine radical mediated process.

The [2 + 2] cycloadditions are concerted reactions that proceed via a cyclic transition state (TS). All bond breaking and bond formation occurs simultaneously, and no intermediates are involved. In the case of formation of a Pyr<>Pyr dimer, the [2 + 2] cycloaddition results in the conversion of two C_5–C_6 π-bonds, one on each moiety, into two σ-bonds (C_5–C_5' and C_6–C_6', respectively).

The textbook example of a [2 + 2] cycloaddition is the cyclodimerization of two molecules of ethylene into one molecule of cyclobutane [14]. Given that the cycloaddition is initiated either thermally or by light the reaction path will, according to the Woodward–Hoffmann rules [15], be

* Corresponding author. Fax: +46-18-511-755.
E-mail address: leif.eriksson@xray.bmc.uu.se (L.A. Eriksson).

1010-6030/02/$ – see front matter
PII: S1010-6030(02)00180-6

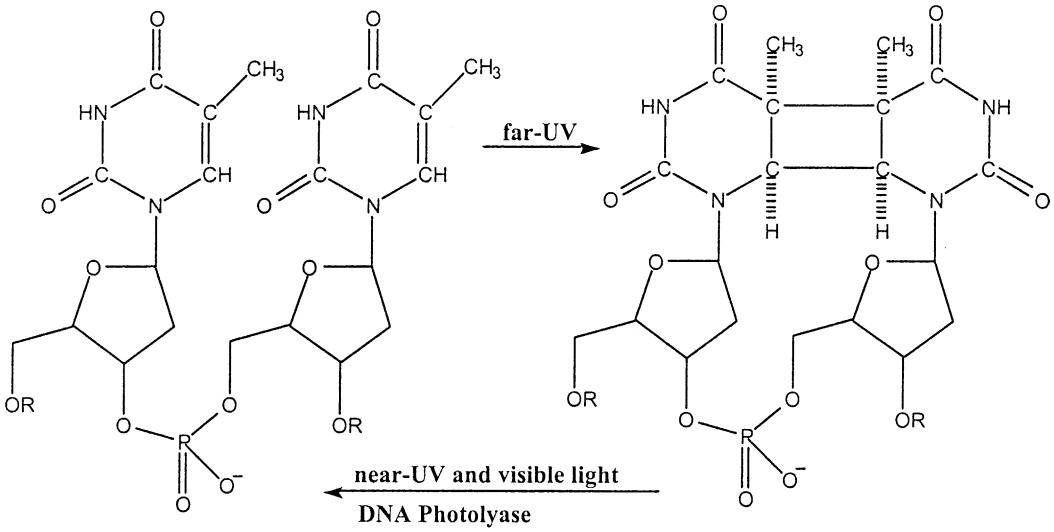

Fig. 1. UV light induced thymine dimer formation (*cis–syn* stereoisomer) between two adjacent thymine bases in the same strand of a DNA molecule. The photoreactivation process is catalyzed by DNA photolyase, which uses near-UV and visible light.

determined by the orbital symmetry of the reactants. In order for the reaction to proceed on the ground state energy surface S_0 (S_0: $\pi_1^2\pi_2^2$), substantial heating is required to overcome a very high activation energy barrier (the formation of cyclobutane from two molecules of ethylene is symmetry-forbidden as a concerted thermal process). If the cyclodimerization is induced photochemically, on the other hand, the reaction initially proceeds along the lowest *singly* excited state surface S_1 (S_1: $\pi_1^2\pi_2\pi_3$). A small energy barrier is then surmounted before the system makes an allowed crossing to the lowest *doubly* excited state surface S_2 (S_2: $\pi_1^2\pi_3^2$). S_2 has a potential energy well—that lies below S_1—at a nuclear configuration that corresponds to a TS structure along the ground state reaction path. This potential energy well, which is the result of an avoided crossing between the S_2 and S_0 states, traps the excited system and serves as a funnel (a leakage channel between S_2 and S_0 [16]) through which the system may either go "forward" to the ground state product (cyclobutane) or "backwards" to the ground state reactants. Thus, the photoinduced cyclodimerization of ethylene does not proceed via an electronically excited product that eventually decays to the ground state through emission of radiation, but proceeds through the decay from S_2 to S_0 at the ground state transition structure.

The photochemical reaction pathway solely involves the *lowest* excited singlet state of the different ethylene–ethylene molecular arrangements along the reaction coordinate. This state initially corresponds to the singly excited S_1 state, but is, as described above, eventually exchanged for the doubly excited S_2 state.

The Woodward–Hoffman rules have, of course, been tested experimentally, and it is well known that photochemically induced [2 + 2] cycloaddition reactions occur readily while they are impossible to initiate thermally under normal conditions. Cycloaddition reactions of small alkenes have also been explored theoretically in some detail, primarily using configuration interaction (CI) or multiconfiguration SCF (MC-SCF) approaches [17–20]. To date, however, no such studies have been made in which systems as large as two pyrimidine bases set to react are investigated. Neither have photochemical reaction studies invoking novel density functional theory (DFT) based approaches been reported. It is, therefore, of interest to investigate the formation of a Pyr<>Pyr dimer utilizing DFT methods. In the present work, we explore both the thermal and the photochemical reaction pathways of a [2 + 2] cycloaddition of pyrimidine bases in DNA. The most common form of pyrimidine dimer found in DNA is that between two thymine bases. In the following, we will hence focus on thymine dimerization and denote the corresponding dimers T<>T.

As mentioned earlier, T<>T dimers may also be produced indirectly from UV irradiation by means of radical addition reactions. The chemistry of these reactions differs considerably from that of cycloadditions. In the case of thymine radicals, we will no longer have localized C_5=C_6 double bonds, and hence the cycloadduct will not be the only reaction product. Since the *cis–syn* cycloadduct is the predominant product detected in UV irradiated DNA, the present study is focused on the reaction between non-radical thymine moieties as a model for UV light induced dimer formation.

We conclude this introduction by noting that the DFT methods employed in this work, for various reasons, will provide only a qualitative estimate of the energetics of the photochemical reaction pathway. First of all, the time-dependent (TD) DFT method used to calculate excitation energies is a single-reference method valid for one-electron processes. Hence, we do not treat doubly excited states (i.e. the S_2 state) *explicitly*. Neither do we optimize the excited state geometries, but compute vertical excitation energies for various structures along the ground

state reaction coordinate. Finally, there is the concern about electron correlation effects at the $S_2 \leftarrow S_0$ avoided crossing. Non-dynamical correlation, that governs interactions between bonding, non-bonding and anti-bonding orbitals, is not explicitly included in the density functionals employed. However, it is included indirectly via the DFT formalism. Dynamic correlation, on the other hand, which is short-range and includes effects of double excitations, is treated explicitly in the LYP correlation functional [21] utilized in the present work. So, albeit a multiconfigurational ab initio approach constitutes a more appropriate (yet time consuming) theoretical foundation to the treatment of electron correlation and a DFT approach is associated with the above mentioned shortcomings, we argue that DFT does in fact include most parts of the effects essential to give a qualitative estimate of the energetics of photochemical reaction processes. We also believe that the results to be presented will provide valuable insight into the process of UV light induced T<>T dimer formation in DNA.

2. Computational details

The computational model of the system under study consisted of two isolated thymine bases. All calculations were carried out using the B3LYP hybrid density functional [22,23] as implemented in the Gaussian 98 program [24]. Geometries were optimized with the 6-31G(d,p) basis set [25]. Based on these geometries, more accurate energies were calculated with the 6-311 G(d,p) and 6-311 + G(d,p) basis sets, respectively [26–28]. The B3LYP/6-311 G(d,p) single point calculations were also performed in conjunction with the polarized continuum model (PCM) [29–31]. The dielectric constant was then chosen to be equal to either 4.335 (to mimic the local environment in DNA), or 78.39 (to mimic the extreme case of free thymine bases in water solution). Frequency calculations were performed at the same level of theory as the geometry optimizations.

Table 1
Key geometric parameters for the stationary points along the thermal reaction pathway

	RC	TS	T<>T
Distances			
C_5–C_5'	4.176[a]	2.339	1.593
C_6–C_6'	4.456[a]	2.123	1.570
C_5–C_6	1.354	1.486	1.551
C_5'–C_6'	1.351	1.414	1.557
Dihedral angles			
C_7–C_5–C_5'–C_7'	35.3[a]	6.8	27.6
N_1–C_6–C_5–C_4	−0.4	−19.9	−29.8
N_1'–C_6'–C_5'–C_4'	0.5	−2.4	−26.1

Distances in Å, dihedral angles in degrees. Obtained at the B3LYP/6-31G (d,p) level.
[a] Held fixed as in the B-DNA X-ray structure of [32].

For the reactant complex (RC), unconstrained geometry optimization of two isolated thymines renders a co-planar structure in which the two bases interact by hydrogen bonds. As this clearly is an unphysical model of neighboring thymines in DNA, we instead chose to optimize the reactant complex with the following constraints (taken from a 1.4 Å resolution X-ray structure of a B-DNA dodecamer [32], and with the atom numbering scheme shown in Fig. 2): $R(C_5–C_5') = 4.18$ Å, $R(C_6–C_6') = 4.46$ Å, and $\angle C_7–C_5–C_5'–C_7' = 35.3°$. The TS and *cis–syn* cycloaddition product (T<>T) structures were obtained through unconstrained geometry optimizations. Frequency calculations were performed in order to identify the stationary points as either minima (RC and T<>T) or a first-order saddle point (TS), and to extract zero-point vibrational energies (ZPE).

Intrinsic reaction coordinate (IRC) calculations [33,34] were subsequently performed (B3LYP/6-31G(d,p) level of theory) in order to follow the thermal reaction path from the

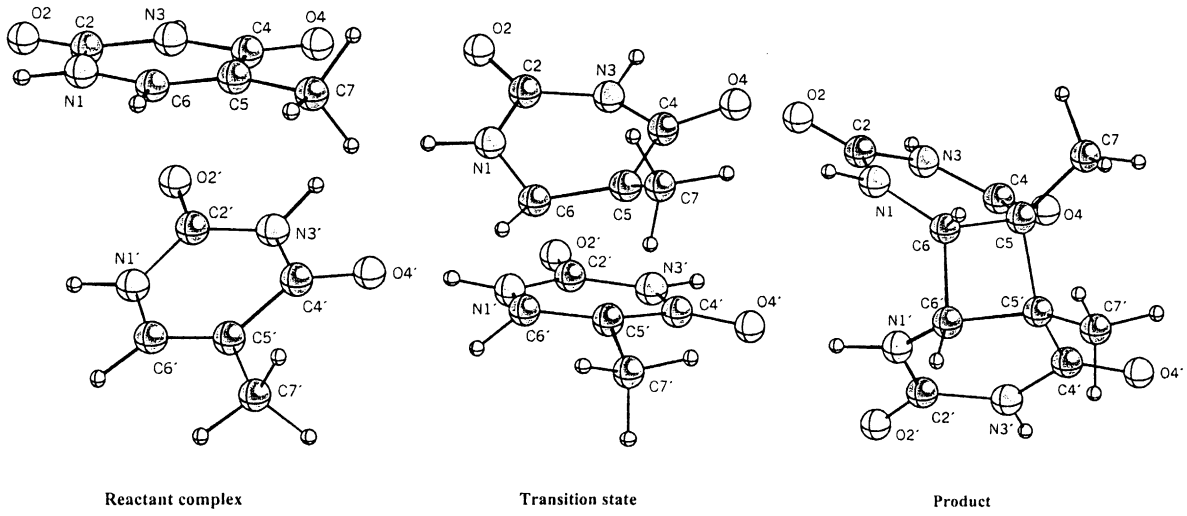

Fig. 2. Geometry optimized structures of stationary points along the thermal reaction pathway. Numerical values are listed in Table 1.

TS towards the reactant complex and the *cis–syn* cycloaddition product, respectively. In geometrical terms, the cycloaddition corresponds to the simultaneous variation of the $R(C_5–C_5')$ and $R(C_6–C_6')$ parameters, respectively. From Table 1 above, we observe that these parameters decrease as 4.18 → 2.34 → 1.59 Å and 4.46 → 2.12 → 1.57 Å, respectively, when the cycloaddition proceeds from the RC to T<>T via the TS. Due to a trade-off between computational effort and the necessity of being able to compute a detailed thermal reaction path, the IRC calculations were restricted to 40 points in each direction. The IRC-structures connecting the TS and the RC did not, however, cover the region close to the RC (all IRC-structures having $R(C_5–C_5') \leq 2.83$ Å and $R(C_6–C_6') \leq 2.69$ Å). Additional structures were, therefore, obtained through constrained geometry optimizations, with the corresponding constraints determined in the following way. From a data set consisting of the $R(C_5–C_5')$, $R(C_6–C_6')$, and $\angle C_7–C_5–C_5'–C_7'$ geometric parameters for the TS, the RC, and the existing IRC-structures "between" TS and RC, linear regression analysis was used to relate $R(C_6–C_6')$ and $\angle C_7–C_5–C_5'–C_7'$ as functions of $R(C_5–C_5')$. The correlation coefficients for the thereby obtained equations were 0.998 and 0.999, respectively. By choosing $R(C_5–C_5') = \{3.00, 3.25, 3.50, 3.75, 4.00$ Å$\}$ and for each choice of $R(C_5–C_5')$, determine the corresponding values of $R(C_6–C_6')$ and $\angle C_7–C_5–C_5'–C_7'$ by using the regression formulae, appropriate constraints were obtained. These constraints were finally used in B3LYP/6-31G(d,p) geometry optimizations of five additional structures connecting the TS and the RC. The IRC calculation in the opposite direction (from the TS towards the T<>T dimer) led to a geometry similar to that of T<>T, and no additional structures were, therefore, needed. Frequency calculations were not performed on any of the IRC structures (see Section 3.1).

Excitation energies were calculated by using the TD-DFT method of Scuseria and co-workers [35]. Since the Gaussian 98 implementation of this method computes vertical excitation energies only, these calculations made use of the ground state geometries of the stationary points and the IRC (+linear regression) structures connecting these. TD-DFT in combination with B3LYP has previously been shown to provide accurate energies for low-lying excited states [36].

3. Results and discussion

3.1. Thermal cycloaddition

The geometry-optimized structures of RC, TS and T<>T are depicted in Fig. 2, and relevant geometric parameters are listed in Table 1.

We observe that the $C_5–C_5'$ and $C_6–C_6'$ distances of the TS—even though the former is somewhat greater than the latter due to steric repulsion between the C_5 methyl groups—both lie within ∼2.1–2.3 Å; a fact that points to a *cyclic* TS. This was confirmed by the vibrational analysis, which showed that the TS structure indeed constitutes a stationary point along a *concerted* reaction path. In addition, the IRC calculation in the region between the TS and the T<>T dimer did not converge to any intermediate (which would suggest a *step-wise* reaction mechanism), but led, as mentioned above, to a geometry similar to that of T<>T. From Table 1, we also note that the cycloaddition induces a puckering of the thymine moieties (cf. the $N_1–C_6–C_5–C_4$ dihedral angles). This feature is the result of the conversion of the $C_5–C_6$ π-bonds into σ-bonds, which is clearly illustrated by the fact that the most puckered thymine moiety of the TS structure (the moiety with $\angle N_1–C_6–C_5–C_4 = -19.9°$) is the one whose $C_5–C_6$ bond has been lengthened the most (from 1.35 to 1.49 Å).

The effects of different computational methodologies on the calculated reaction energy (ΔE) and energy barrier ($\Delta E^{\dagger}$) for the thermal cycloaddition are presented in Table 2. We note that the effect of including ZPE corrections to ΔE and $\Delta E^{\dagger}$ is small ($\Delta\Delta E = 2.2$ kcal/mol and $\Delta\Delta E^{\dagger} = -1.7$ kcal/mol). ZPE corrections were for this reason not calculated on any of the IRC structures, and are in the following not taken into account. As for the single point energy calculations, the data shows that adding one set of diffuse functions to the 6-311 G(d,p) basis set implies only minor changes of the calculated values of ΔE and $\Delta E^{\dagger}$ ($\Delta\Delta E = -0.2$ kcal/mol and $\Delta\Delta E^{\dagger} = -1.0$ kcal/mol), and that solvation effects are more pronounced when the dielectric constant equals that of bulk water ($\Delta\Delta E = -6.9$ kcal/mol and $\Delta\Delta E^{\dagger} = -6.9$ kcal/mol when $\varepsilon = 78.39$, whereas $\Delta\Delta E = -3.0$ kcal/mol and $\Delta\Delta E^{\dagger} = -3.4$ kcal/mol when $\varepsilon = 4.335$). Based on these results, the ground state single point energy calculations on the IRC (+linear regression) structures were solely carried out at the B3LYP/6-311 G(d,p) level in vacuo and embedded in a polarizable continuum with $\varepsilon = 78.39$.

We conclude this section by emphasizing that at all levels of theory employed a thermally induced cyclodimerization is associated with a barrier of >80 kcal/mol, making this pathway energetically inaccessible. Furthermore, the fact that the reaction energy amounts to >13 kcal/mol clearly shows that this reaction will not take place. It should, however, be noted that thymine dimerization may proceed in a non-photochemical fashion if one considers *step-wise* reaction mechanisms as well. An ab initio MC-SCF study of Robb and co-workers [19] showed, as an interesting comparison in this context, that while a thermal supra-antara [2 + 2] cycloaddition of two molecules of ethylene into one molecule of cyclobutane proceeds via a TS that lies 87.9 kcal/mol above the two ethylenes, the barriers associated with a step-wise pathway involving fragmentation of either a *gauche* or a *trans*-tetramethylene diradical intermediate are less than 1 kcal/mol.

Table 2
Energies of the thermal reaction pathway (kcal/mol)

	6-31 G(d,p)	6-31 G(d,p) ZPE	6-311 G(d,p)	6-311 G(d,p) PCM;		6-311 + G(d,p)
				$\varepsilon = 4.334$	$\varepsilon = 78.39$	
ΔE	18.0	20.2	20.2	17.2	13.3	20.0
$\Delta E^{\dagger}$	87.6	85.9	87.5	84.1	80.6	86.5

All calculations carried out with the B3LYP functional, using B3LYP/6-31 G(d,p) optimized geometries. The reaction energy (ΔE) is calculated as $\Delta E = E(\text{T}\diamond\text{T}) - E(\text{RC})$; the activation energy barrier ($\Delta E^{\dagger}$) is calculated as $\Delta E^{\dagger} = E(\text{TS}) - E(\text{RC})$. ZPE corrections are excluded unless otherwise explicitly noted.

3.2. Photochemical cycloaddition

The energies corresponding to the *lowest* excited singlet state of RC, TS, and T◇T are listed in Table 3. The excitation energy for the RC corresponds to the $S_1 \leftarrow S_0$ transition, and equals 4.5–4.7 eV (264–276 nm), which is within the far-UV region (200–300 nm) known to induce the formation of cyclobutane pyrimidine dimers [1,2] The excitation energy for the TS, on the other hand, corresponds to the $S_2 \leftarrow S_0$ transition and is only 0.7 eV, whereas the excitation energy for the T◇T dimer increases to 4.9–5.0 eV due to the conversion of the C_5–C_6 π-bonds into σ-bonds. This implies that any repair process involving direct excitation of the dimer would require additional energy and hence even shorter wavelengths. Nature has, however, instead chosen to repair these damages, i.e. split the dimers, by means of DNA photolyases that function in the near-UV–VIS (300–500 nm) range of the spectrum [3–5]. These enzymes make use of two non-covalently bound cofactors—one light-harvesting cofactor and one catalytic cofactor—to reduce the T◇T dimer and form the T◇T radical anion, which decomposes readily [6–9].

The data presented in Table 3 shows that adding one set of diffuse functions to the 6-311 G(d,p) basis set only has a small effect on calculated excitation energies. The excited state single point energy calculations on the IRC (+linear regression) structures were, therefore, carried out at the same levels as the corresponding ground state calculations. The results are shown in Fig. 3. Even though the fact that we do not optimize the excited state geometries obviously means that the curves representing the photochemical reaction pathway should not, strictly speaking, be viewed as potential energy curves, we observe the presence of a "potential energy" well at a nuclear configuration corresponding to the TS along the thermal reaction pathway. Interestingly, an energy barrier of 3–4 kcal/mol only is needed before the system reaches this minimum, which clearly shows that the photochemical reaction pathway, as opposed to the thermal reaction pathway with its barrier of 80–88 kcal/mol, is energetically feasible. We further note from Fig. 3 that the gap between the two curves at the leakage channel is 12–16 kcal/mol, and that the use of the PCM for treating solvation effects do not significantly alter the overall in vacuo energies of the two reaction pathways.

As already mentioned, the TD-DFT approach used to investigate the photochemical reaction pathway has limitations that, together with the fact that experimental data is largely unavailable, makes it somewhat difficult to judge the estimate of the associated barrier. In order for the reaction to proceed within a photochemically reasonable period of time, this barrier should be small. It is, thus, encouraging that the calculations predict a barrier of 3–4 kcal/mol only. In this context, the results of an early ab initio study of the photochemical disrotatory closure of butadiene to cyclobutene are interesting [18]. The mechanistic details of this reaction are similar to those of a [2 + 2] cycloaddition and, on the basis of CI calculations, these researchers reported a barrier of 5–8 kcal/mol, which agrees well with the present data. The size of the gap between the two curves at the leakage channel is also a key feature of the type of reaction mechanism under investigation here. Even though other factors certainly come into play as well, the probability for the system to undergo the $S_2 \leftarrow S_0$ transition—which in a two-state model for avoided crossings would be given by the Landau–Zener formula [37,38]—depends on this gap not being too large. As for the cyclization of butadiene to cyclobutene, the gap was estimated to be of the order of

Table 3
Vertical excitation energies for the stationary points along the thermal reaction pathway (eV)[a]

	6-311 G(d,p)	6-311 G(d,p) PCM $\varepsilon = 4.335$	6-311 G(d,p) PCM $\varepsilon = 78.39$	6-311 + G(d,p)
RC	4.67	4.67	4.53	4.61
TS	0.69	0.68	0.69	0.71
T◇T	4.96	5.02	5.03	4.91

The state under investigation is the *lowest* excited singlet state.
[a] A1l calculations carried out with the B3LYP functional.

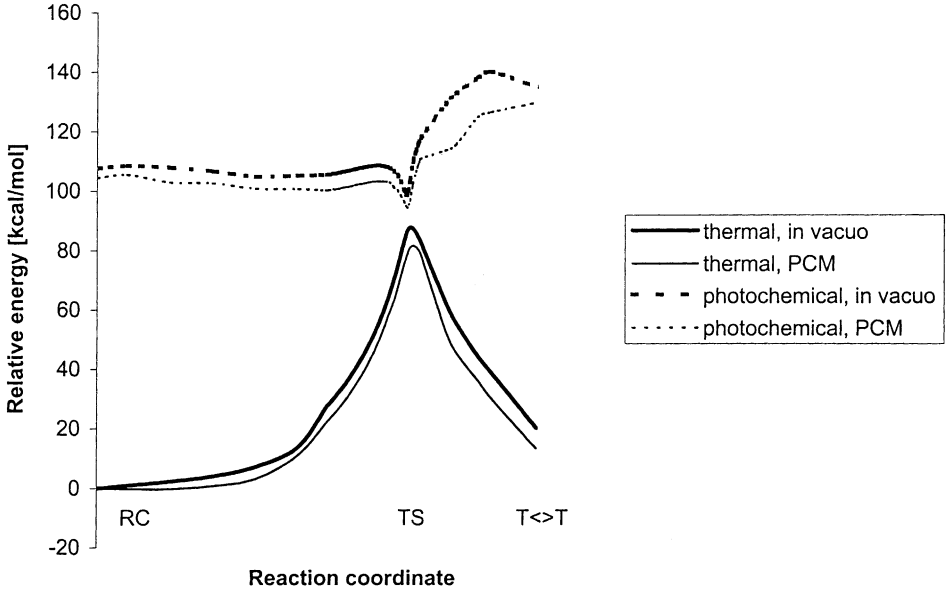

Fig. 3. Potential energy curves for the thermal and the photochemical reaction pathway. The photochemical pathway solely involves the *lowest* excited singlet state of the different molecular arrangements along the reaction coordinate. Energies are given relative to the RC.

20–25 kcal/mol [18], which is 4–13 kcal/mol larger than our result.

4. Conclusions

We have in the present work explored the formation of thymine dimers in DNA using DFT methods. Starting from the orientation of two thymine residues in B-DNA, the potential energy surface corresponding to a cycloaddition reaction mechanism was computed. It was thereby found that a very high activation energy barrier makes it impossible to initiate the cycloaddition thermally, and also that the overall reaction energy excludes the possibility of a thermal reaction pathway.

Next, the energies of a photochemically initiated cycloaddition reaction was investigated. On the basis of ground state geometries, the energy surface for a reaction proceeding via the lowest excited singlet state of the different molecular structures along the reaction coordinate was calculated using TD-DFT. The results then obtained clearly showed that a photochemical reaction pathway, as opposed to a thermal reaction pathway, is energetically feasible, since an energy barrier only a few kilocalories per mol needs to be surmounted. The calculations on the reactant complex furthermore showed that the vertical excitation energy corresponding to the $S_1 \leftarrow S_0$ transition ($\pi \rightarrow \pi^*$) lies in the far-UV region, in accordance with experimental data. Altogether, these findings serve as an illustrative example of how UV radiation may induce DNA lesions. The fact that the calculations provide a “potential energy” curve for the photochemical reaction pathway that, at least qualitatively, displays the anticipated features moreover indicates that TD-DFT is a promising tool to be used in future studies of photochemical reaction processes.

Acknowledgements

The Swedish Research Council (VR), is gratefully acknowledged for financial support. Grants of computing time at the supercomputing facilities in Linköping (NSC) and Stockholm (PDC) are also gratefully acknowledged.

References

[1] S.Y. Wang, Photochemistry and photobiology of nucleic acids, Chemistry, Vol. I, Academic Press, San Diego, CA, 1976.
[2] W. Harm, Biological Effects of Ultraviolet Radiation, Cambridge University Press, Cambridge, 1984.
[3] A. Sancar, G.B. Sancar, Ann. Rev. Biochem. 57 (1988) 29–67.
[4] G.B. Sancar, Mutat. Res. 236 (1990) 147–160.
[5] B. van Houten, A. Snowden, BioEssays 15 (1993) 51–59.
[6] A. Sancar, Biochemistry 33 (1994) 2–9.
[7] P.F. Heelis, R.F. Hartman, S.D. Rose, Chem. Soc. Rev. 24 (1995) 289–297.
[8] T. Carell, L.T. Burgdorf, L.M. Kundu, M. Cichon, Curr. Opin. Chem. Biol. 5 (2001) 491–498.
[9] B. Durbeej, L.A. Eriksson, J. Am. Chem. Soc. 122 (2000) 10126–10132.
[10] J.-S. Taylor, D.S. Garrett, I.R. Brockie, D.L. Svoboda, J. Telser, Biochemistry 29 (1990) 8858–8866.
[11] K. McAteer, Y. Jing, J. Kao, J.-S. Taylor, M.A. Kennedy, J. Mol. Biol. 282 (1998) 1013–1032.
[12] K. Miaskiewicz, J. Miller, M. Cooney, R. Osman, J. Am. Chem. Soc. 118 (1996) 9156–9163.
[13] T.I. Spector, T.E. Cheatham III, P.A. Kollmann, J. Am. Chem. Soc. 119 (1997) 7095–7104.
[14] A. Gilbert, J. Baggott, Essentials of Molecular Photochemistry, Blackwell, Oxford, 1991.

[15] R.B. Woodward, R. Hoffmann, J. Am. Chem. Soc. 87 (1965) 395–397.
[16] J. Michl, Top. Curr. Chem. 46 (1974) 1–59.
[17] W. Th, A.M. van der Lugt, L.J. Oosterhoff, J. Am. Chem. Soc. 91 (1969) 6042–6049.
[18] D. Grimbert, G. Segal, A. Devaquet, J. Am. Chem. Soc. 97 (1975) 6629–6632.
[19] F. Bernardi, A. Bottoni, M.A. Robb, H.B. Schlegel, G. Tonachini, J. Am. Chem. Soc. 107 (1985) 2260–2264.
[20] F. Bernardi, A. Bottoni, M.A. Robb, A. Venturini, J. Am. Chem. Soc. 112 (1990) 2106–2114.
[21] C. Lee, W. Yang, R.G. Parr, Phys. Rev. B 37 (1988) 785–789.
[22] A.D. Becke, J. Chem. Phys. 98 (1993) 5648–5652.
[23] P.J. Stephens, F.J. Devlin, C.F. Chabalowski, M.J. Frisch, J. Phys. Chem. 98 (1994) 11623–11627.
[24] M.J. Frisch, G.W. Trucks, H.B. Schlegel, G.E. Scuseria, M.A. Robb, J.R. Cheeseman, V.G. Zakrzewski, J.A. Montgomery, R.E. Stratmann, J.C. Burant, S. Dapprich, J.M. Millam, A.D. Daniels, K.N. Kudin, M.C. Strain, O. Farkas, J. Tomasi, V. Barone, M. Cossi, R. Cammi, B. Mennucci, C. Pomelli, C. Adamo, S. Clifford, J. Ochterski, G.A. Petersson, P.Y. Ayala, Q. Cui, K. Morokuma, D.K. Malick, A.D. Rabuck, K. Raghavachari, J.B. Foresman, J. Cioslowski, J.V. Ortiz, B.B. Stefanov, G. Liu, A. Liashenko, P. Piskorz, I. Komaromi, R. Gomperts, R.L. Martin, D.J. Fox, T.A. Keith, M.A. Al-Laham, C.Y. Peng, A. Nanayakkara, C. Gonzalez, M. Challacombe, P.M.W. Gill, B.G. Johnson, W. Chen, M.W. Wong, J.L. Andres, M. Head-Gordon, E.S. Replogle, J.A. Pople, Gaussian 98, Rev. A.7, Gaussian Inc., Pittsburgh, PA, 1998.
[25] P.C. Hariharan, J.A. Pople, Theor. Chim. Acta 28 (1973) 213–222.
[26] R. Krishnan, J.S. Binkley, R. Seeger, J.A. Pople, J. Chem. Phys. 72 (1980) 650–654.
[27] A.D. McLean, G.S. Chandler, J. Chem. Phys. 72 (1980) 5639–5648.
[28] M.J. Frisch, J.S. Binkley, J.A. Pople, J. Chem. Phys. 80 (1984) 3265–3269.
[29] S. Miertus, E. Scrocco, J. Tomasi, Chem. Phys. 55 (1981) 117–129.
[30] J. Tomasi, M. Persico, Chem. Rev. 94 (1994) 2027–2094.
[31] C.J. Cramer, D.G. Truhlar, Chem. Rev. 99 (1999) 2161–2200.
[32] X. Shui, L. McFail-Isom, G.G. Hu, L.D. Williams, Biochemistry 37 (1998) 8341–8355.
[33] C. Gonzalez, H.B. Schlegel, J. Chem. Phys. 90 (1989) 2154–2161.
[34] C. Gonzalez, H.B. Schlegel, J. Phys. Chem. 94 (1990) 5523–5527.
[35] R.E. Stratmann, G.E. Scuseria, M.J. Frisch, J. Chem. Phys. 109 (1998) 8218–8224.
[36] D.J. Tozer, N.C. Handy, J. Chem. Phys. 109 (1998) 10180–10189.
[37] L. Landau, Phys. Z. U.S.S.R. 1 (1932) 426.
[38] C. Zener, Proc. R. Soc., London Ser. A 137 (1932) 696–702.